ANALYSIS AND MONITORING OF CAGE DYNAMICS IN BALL BEARINGS FOR SPACE APPLICATIONS

Massimo Palladino[(1)], Silvio Giuseppe Neglia[(1)], Marcin Wygachiewicz[(2)]

[(1)]ESA-ESTEC, Keplerlaan 1, 2200 AG Noordwijk ZH (The Netherlands), Email: Massimo.Palladino@esa.int

[(2)]Sener Poland, al. Jerozolimskie 202, 02-486 Warszawa (Poland), Email: Marcin.Wygachiewicz@sener.pl

ABSTRACT

The literature is rather limited for what concerns prediction methods and test measurements of the cage dynamic motion in ball bearings for space applications. More specifically, some commercial software exists in the US (ADORE from PKG, which is delivered to several European companies like SAGEM or SNECMA) or is company proprietary (BEAST from SKF). In addition, the High Speed Camera monitoring of the cage has been introduced already in some industrial applications (see ref.[1] for an application in China and ref.[2] for an application in Latvia) but has never been used to derive the cage dynamics in a ball bearing for space applications.
The present study aims at:

- Introducing in Europe a relatively simple (and free) code developed in MATLAB to analyse a ball bearing design and conclude on the stability/instability of the cage.
- Gain experience in Europe with the usage of a High Speed Camera to monitor the cage motion and conclude by test on the stability/ instability in the given application.

Particularly, a ball bearing, typically used in space mechanisms, is analysed with the software developed by the European Space Agency (ESA). The same bearing is also tested and monitored with a High Speed Camera. A model/ test correlation is attempted and globally demonstrates that a relatively simple (and cheap) model, coupled with a test using a High Speed Camera are suitable tools to conclude on the stability/ instability of the ball bearing cage.

1. INTRODUCTION

Despite of the existence of some models that describe the in-plane motion of a bearing cage for angular contact bearings (i.e. operating in the EHD lubrication regime), the phenomena connected with ball bearings cage instability issues, ball bearing kinematics and dynamics are still not fully known. The most popular models available for simulations of ball bearings include:

- Kannel's model,
- Boesiger's model (Boesiger & Warner, n.d.),
- Mevel's model,
- Harris' model (Harris & Kotzalas, 2007),
- Meeks' model.

In practice, commercial software, also based on these models, is available in the US and is used also by European companies. Some other software is company proprietary. The consequences are:

- On one hand, the actually implemented code is not easily accessible, making these commercial codes rather fuzzy.
- On the other hand, it is not clear to the public that these codes have been correlated with test results.

Therefore, it is not that obvious to conclude that the bearing cage dynamics are known to the space mechanisms world.
In the present paper, taking advantage of a student placement for a stage (Mr.Silvio Neglia) and of an ESA YGT in the mechanisms section (Mr. Marcin Wygachiewicz), it has been tried at ESA-ESTEC to improve the understanding of the ball bearing cage dynamics by:

- Developing an in-house MATLAB code based on an in-plane analysis of the cage motion considering interaction with the inner/ outer races and the balls. For every contact, a normal force and a tangential force are evaluated. The normal force depends on the stiffness of the contact (as based on the Hertzian theory) and on a damping coefficient (allowing to dissipate some energy during the contact). The tangential force depends on a friction coefficient and on the normal force. Particularly, the friction coefficient is chosen as being the "pin-on-disc" measured friction coefficient for the contact cage/ inner/ outer races (where there is mainly sliding) and the

"spiral orbit tribometer" measured friction coefficient for the contact cage/ balls (where there is sliding/ rolling). From these forces, resultant force/ moment respectively at/ around the centre of gravity of the cage/ balls are computed. From the resultant forces/ moments, the motion of the cage/ balls is determined by using analytical mechanics equations.

- Ball bearing tests have been performed at ESTL (UK) by varying fundamental parameters (bearing speed and lubricant presence/ not presence). The amount of money allocated to this activity was small (<50 kEuros). Therefore, only one type of bearing (EX25) was available. Also, that is why only the speed and the lubricant presence/ not presence have been the modified parameters.
- Thanks to the ESA-ESTEC high-speed camera, it was possible to appropriately monitor the cage motion. Recording and analysing the cage motion allowed to correlate the MATLAB model.
- Results of this activity are used as inputs in a currently running ESA GSTP with the ULG (Belgium) to improve the MATLAB model.
- As a future activity, once the MATLAB will be improved and further correlated through the GSTP activity, the following will be considered:
  - An output of the model is the number of contacts cage/ balls.
  - The current work done by ESTL (through an ESA-ESTEC TAP activity) on the fundamentals of transfer films lubrication (see ref.[3]) aims at obtaining cage wear from the number of contacts cage/ balls.
  - There is an on-going ESA-ESTEC ARTES 5.1 activity with AAC (Austria) to develop a European self-lubricating material for ball bearing cages, replacing the US Duroid and PGM-HT.
  - Putting all these previous points together, it will be possible to get a European model to predict the life of a self-lubricating ball bearing cage (based on the GSTP, TAP and ARTES 5.1 ESA activities). It is believed this might be a breakthrough in space mechanisms science as this has not been done at the best author's knowledge.

2. MODELLING CONSIDERATIONS

2.1. Basic equations of the planar cage dynamics

The cage motion is described in the following reference axes system:

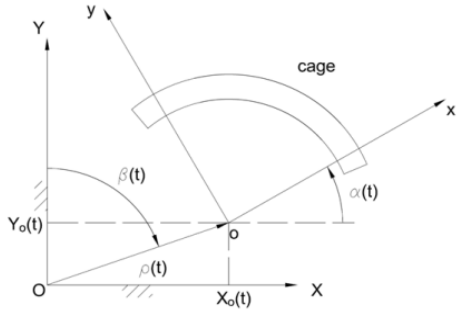

Figure 1: Motion of the cage – reference axes

Considering the resultant forces at the centre of gravity and the moment around the centre of gravity, the cage equations (for the 3 in-plane degrees of freedom) are:

$$\begin{cases} I_z\ddot{\alpha} = M_z \\ M_c\left[sin\beta\left(\ddot{\rho} - \rho\dot{\beta}^2\right) + cos\beta\left(\rho\ddot{\beta} + 2\dot{\rho}\dot{\beta}\right)\right] = F_x \\ M_c\left[cos\beta\left(\ddot{\rho} - \rho\dot{\beta}^2\right) + sin\beta\left(\rho\ddot{\beta} + 2\dot{\rho}\dot{\beta}\right)\right] = F_y \end{cases} \quad (1)$$

where: I_z – approximate moment of inertia for the ball bearing's cage, M_c is the mass of the cage, M_z is the moment acting on the cage (due to the several impacts with the races/ balls), F_x and F_y are the resultant forces acting respectively in X and Y

The mentioned contact situations are described in the following sections.

2.2. Contact cage / races

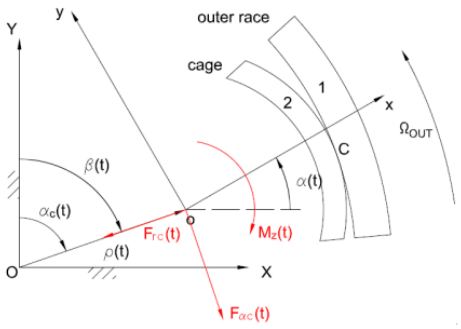

Figure 2: Contact cage / outer race

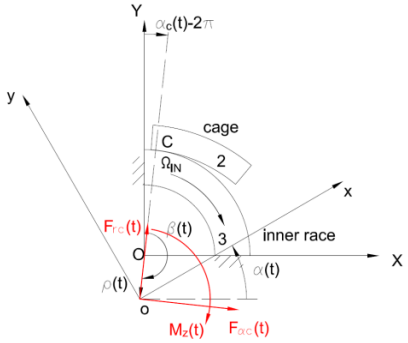

Figure 3: Contact cage / inner race

F_{rc} and $F_{\alpha c}$ are the forces acting on the cage in the local reference system oxy. $F_{\alpha c}$ induces a torque contribution to the cage. The torque contribution is:

$$M_z = -F_{\alpha c} R_c \ (for\ outer\ race\ guided\ bearing)$$
$$M_z = -F_{\alpha c} r_c \ (for\ inner\ race\ guided\ bearing) \quad (2)$$

where: R_c – outer radius of the cage; r_c – inner radius of the cage.

The normal force F_{rc} is composed of two terms:

- The first one is due to the stiffness in the contact.

$$C_{sr}(\rho - \rho_m) \quad (3)$$

where: C_{sr} – stiffness between cage and race (outer or inner race).

- The second one is due to the damping in the contact. This term is dependent on the speed $\dot{\rho}$ in the contact. The damping coefficient C has been set arbitrarily to 50 N sec/m. This value can be tuned later to correlate the model with test results.

$$C\dot{\rho} \quad (4)$$

The tangential force $F_{\alpha c}$ depends on the friction force in the contact and the normal force. The following applies:

$$F_{\alpha c} = f_{cr} F_{rc} = f_{cr}[C_{sr}(\rho - \rho_m)] \quad (5)$$
$$f_{cr} = -f_{POD} sgn[v_{C,rel}] \quad (6)$$

The friction coefficient in the contact cage/ races is measured by a pin-on-disc test. The pin-on-disc friction coefficient is chosen because in this contact there is mainly sliding.

The detection of the cage/ races contact is done without any specific assumption. The condition for contact is:

$$\rho \geq \rho_m \quad (7)$$

Outer and inner race guided bearing cases are distinguished as follows:

- outer race guided bearing: if $r_o - R_c < r_c - R_i \overset{then}{\Longrightarrow} \rho_m = r_o - R_c$,
- inner race guided bearing: if $r_o - R_c > r_c - R_i \overset{then}{\Longrightarrow} \rho_m = r_c - R_i$,

where: r_o – inner radius of the outer ring; R_c – outer radius of the cage; r_c – inner radius of the cage; R_i – outer radius of the inner race.

2.3. Contact cage / balls

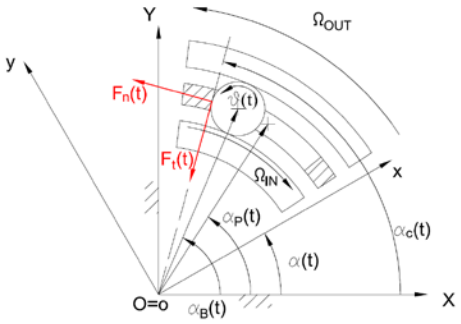

Figure 4: Contact cage/ balls

The normal force F_n has two components:

- The first one is due to the stiffness C_{sl} in the contact (based on Hertzian theory).

$$C_{sl}\delta_b = C_{sl}[\alpha_B - \alpha_P]R_p \quad (8)$$

where: α_B – angular position of the ball; α_P – angular position of the cage pocket; R_p – ball bearing pitch radius;

- The second one is due to the damping existing in the contact. Also in this case a damping coefficient C of 50 N sec/m is deliberately chosen and can be tuned during the model correlation with the test results.

$$C[\dot{\alpha_B} - \dot{\alpha_P}]R_P \quad (9)$$

The tangential force depends on the friction coefficient at the contact and the normal force:

$$F_t = f_{cb} F_n = f_{SOT} F_n \quad (10)$$

In this case, the friction coefficient measured during a spiral orbit tribometer test is preferred because the nature of the contact cage/ ball involves both rolling and sliding. The spiral orbit tribometer test, performed at ESTL, is more indicated to evaluate the relevant friction coefficient.
The normal force F_n induces a torque contribution on the cage as follows:

$$M_z = F_n R_c \quad (11)$$

M_z has a positive value in case of a front cage/ ball contact and a negative value in case of a back cage/ ball contact.
The detection of a cage/ ball contact includes a simplification. In fact, cage/ ball detection is based on the following:

$$|\alpha_B - \alpha_P| R_p \geq \frac{d}{2} \quad (12)$$

where: α_B – angular position of the ball; α_P – angular position of the cage pocket; R_p – ball bearing pitch radius; d – dimension of the cage pocket.

The underlying simplification is that, when checking the cage/ ball contact, the cage centre is considered located at the bearing centre. According this approximation, the cage/ ball contact occurs around a circumference of radius R_p. This assumption is justified based on the fact that, in a ball bearing, the cage radial displacement is very small compared to the bearing diameter.

2.4. Balls motion

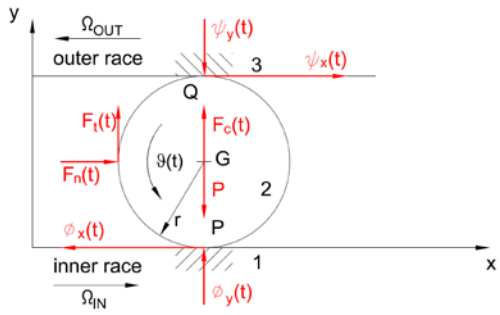

Figure 5: Forces acting on the balls

Forces acting on the ball shown in Figure 5 represent:

- F_c – centrifugal force
- ψ_x – friction force between outer race and ball
- ψ_y – normal force between outer race and ball
- F_n – normal force between cage and ball
- F_t – tangential force between cage and ball
- ϕ_x – friction force between inner race and ball
- ϕ_y – normal force between inner race and ball
- P – force due to the gravity

In practice, P = 0 (no gravity) and ψ_y is in fact the bearing's preload.

Pure stick motion or stick-slip motion are possible. However, for space ball bearings, only pure stick motion is in principle applicable (because of the preload). This translates into:

$$\begin{cases} v_{P,2} = v_{P,1} \\ v_{Q,2} = v_{Q,3} \end{cases} \quad (13)$$

Considering that pure stick occurs when:

- the external forces acting on the ball are in absolute value bounded by the friction force,
- the torque acting on the ball is in absolute value bounded by the friction torque,
- there is no relative velocity between the ball and the races,

the following is derived:

$$\begin{cases} \dot{x} = \frac{R_i(\Omega_{out}-\Omega_{in})+2R_B\Omega_{out}}{2} \\ \dot{\vartheta}_B = \frac{R_i(\Omega_{out}+\Omega_{in})+2R_B\Omega_{out}}{2R_B} \\ |F_n| < \phi_x - \psi_x \\ |F_t|R_B < (-\phi_x - \psi_x)R_B \end{cases} \quad (14)$$

where:

$$\begin{cases} \psi_x = f_{SOT} \cdot \psi_y \\ \phi_x = f_{SOT} \cdot \phi_y \end{cases} \quad (15)$$

Spiral orbit tribometer measurements are used also in this case as this type of tribometer, available at ESTL, tends to represent the type of contact appearing between a ball and races inside a ball bearing.

In case the pure stick conditions are violated, then the stick-slip associated equations are available in the MATLAB code.

3. MATLAB code results

To get a first flavour on the MATLAB code results, an EX25 ball bearing was simulated lubricated (with Fomblin Z25) and unlubricated at a speed of 2000 RPM. These are the results found before any correlation with test:

<u>EX25 unlubricated</u>
In this case, based on available data from previous measurements:

- F_{POD} = 0.22
- F_{SOT} = 0.185

The following cage centre trajectory is found (in 0.5 sec → more than five cage rotations are done):

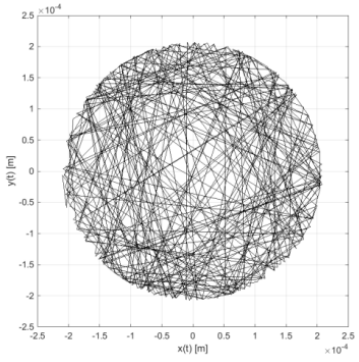

Figure 6: EX25 unlubricated at 2000 RPM

<u>EX25 lubricated</u>
In this case, based on available data from previous measurements:

- F_{POD} = 0.12
- F_{SOT} = 0.085

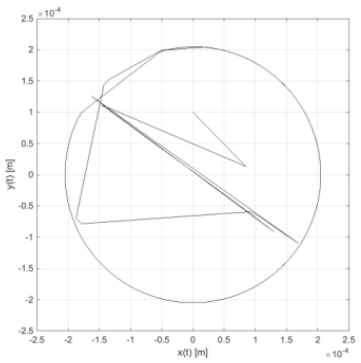

Figure 7: EX25 lubricated at 2000 RPM

The code seems to indicate stability when the ball bearing is properly lubricated (and it coincides with the expected behaviour).

4. High speed camera test results

In order to verify and correlate the numerical model with the real test data, a short test campaign was performed at ESTL. High speed camera measurement was chosen in order to check its applicability to bearing's cage monitoring application (only laser vibrometer tests were carried out in the past by ESTL).

4.1. Test set-up

Tests have been performed by using a dedicated bench allowing testing a pair of preloaded bearings as shown hereafter:

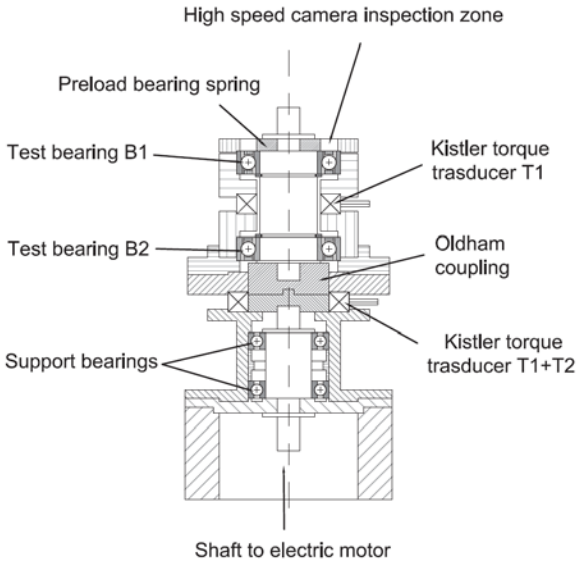

Figure 8: Ball bearing test bench at ESTL

Kistler torque transducers allow direct measurement of torque of the upper bearing and sum of torques of the upper and lower bearing.

The ESA High Speed Camera was installed above the upper bearing as shown in the following figure.

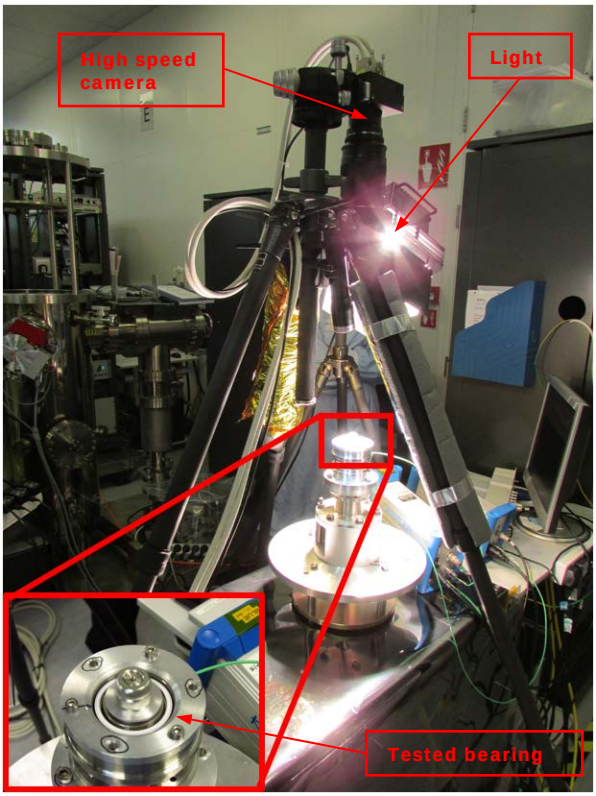

Figure 9: ESA High Speed Camera test stand configuration

A marker was glued on the cage with binary coded angular marks and a circumferential mark to help detecting the trajectory of the cage.

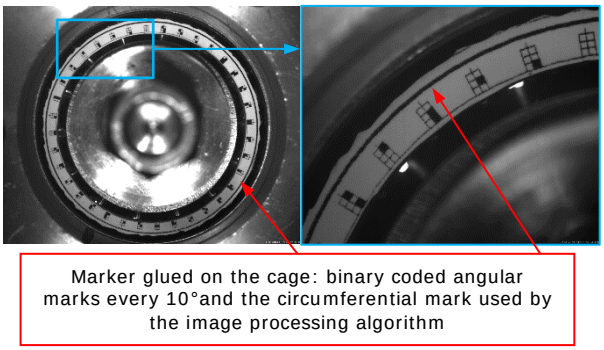

Figure 10: Recorded bearing's cage

The Basler 504k High Speed Camera recorded images with resolution of up to 1280x1024 pixels, speed up to 500 frames/sec. It allowed for the maximum pixel size of corresponding to 12µm x 12µm. The camera's FOV was adjusted to record full cage or cage segment (Figure) by using two types of lenses.

Two preloaded (150 N) bearing pairs of EX25 were tested (one pair lubricated and one pair unlubricated).

Bearings	Preload (N)	Oil [µl]	Oil	No. of balls
Pair 1	150	0	None	14
Pair 2	150	40	Z25	14

Table 1: Bearing pairs descriptions

Parameters of the outer race	
Material	AISI 52100 Steel
Land diameter	0.03991 [m]
Outer diameter	0.04700 [m]
Parameters of the inner race	
Material	AISI 52100 Steel
Land diameter	0.03210 [m]
Inner diameter	0.02500 [m]
Parameters of the balls	
Material	AISI 52100 Steel
Diameter	0.00635 [m]
Number of balls	14
Parameters of the cage	
Material	Phenolic resin Tufnell RLF-1
Outer diameter	0.03950 [m]
Inner diameter	0.03450 [m]
Diameter of the pocket	0.00670 [m]
Parameters of lubricant	
Lubricant type	Z25 Fomblin
Other parameters	
Contact angle	15 [˚]
Axial preload	150 [N]

Table 2: EX25 description

4.2. Ball bearing tests performed

The 60, 1440 and 2000 RPM tests were performed with the HSC monitoring of the upper bearing. Variable frequency – number of frames per second was selected in order to observe a particular angle change on the consecutive frames, i.e.:

- 60 [RPM] (150 [Hz] – allowed to observe ≈1[˚] of cage rotation every frame; 15[Hz] – allowed to observe ≈10[˚] of cage rotation every frame),
- 1440 [RPM] (360 [Hz] – allowed to observe ≈10[˚] of cage rotation every frame),
- 2000 [RPM] (500 [Hz] – allowed to observe ≈10[˚] of cage rotation every frame).

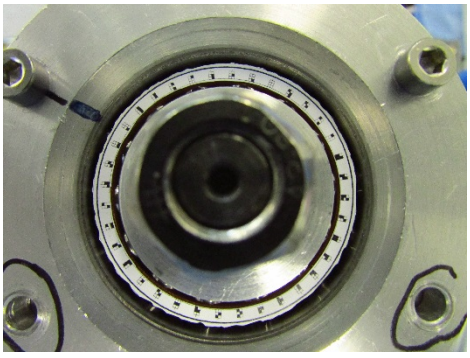

Figure 11: Image of the upper bearing assembled on the test bench

4.3. Analysis of the HSC images

The images obtained with the HSC were processed with numerical image processing techniques implemented in MATLAB (Image Processing Toolbox).

The results give the estimation of the cage centre position for each frame and the cage relative rotation. These give time signals of the cage's three degrees of freedom that are then used to correlate the recordings with the numerical model.

A brief explanation of the image processing algorithm is presented in the following subsections.

4.3.1. Pre-processing

The image is modified for objects identification through the following steps:

- Edge detection (FFT and gradient magnitude of the frame).

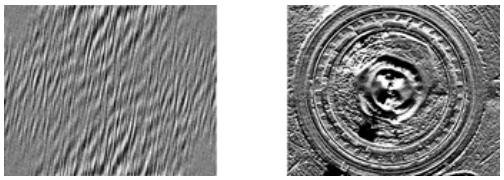

Figure 12: FFT and gradient magnitude (edge detection)

- Mask application in order to obtain only circumferential and angular patterns.

Figure 13: Mask application

Lines thinning to 1 pixel and final adjustments are performed at the end of the pre-processing.

4.3.2. Processing

This phase represents the actual circle detection and consists of:

- Circle detection based on MATLAB built-in and other algorithms.

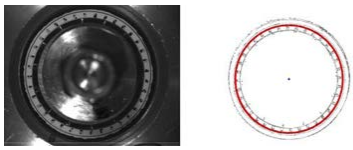

Figure 14: Circle detection

As a result the centre of the cage coordinates with respect to the centre of the image as well as the relative rotation of the cage is determined.

4.3.3. Post-processing

This last phase acquires, manipulates and cleans the output data. It consists of:

- Filtering of the signals (anti-aliasing filter).
- Numerical differentiation of the signals (for the cage velocities).
- Error adjustment (based on the measured deviation between the centres of the cage and the glued cage mark).
- FFTs and PSDs of the filtered signals.

4.4. Test results

Test results are presented, as an example, for 1440 RPM.

The following figures represent the cage centre trajectory for the unlubricated and lubricated cases for the first 150 frames, knowing that the frame rate is 360 Hz:

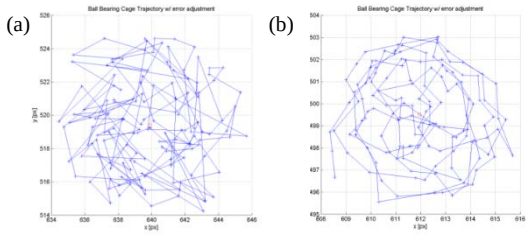

Figure 15: Cage's trajectory: (a) unlubricated, (b) lubricated

The measurements obtained with the Kistler torque transducers are shown hereafter:

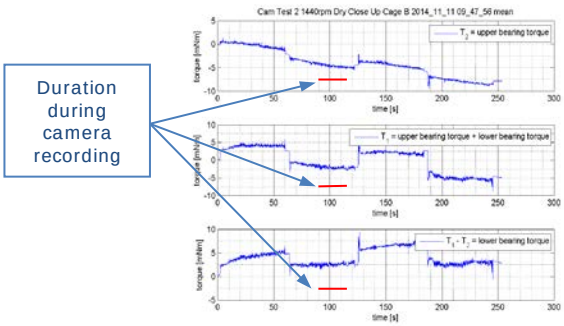

Figure 16: Torque measurements: (a) unlubricated, (b) lubricated

No significant torque fluctuation is seen at 1440 RPM for the unlubricated case, indicating in fact no evidence of cage instability. On the other hand results of the image processing (and visual check of the recorded videos) indicate a less noisy behaviour of the cage which is related with the presence of lubrication. In the case without lubrication, the bearing's cage shows more erratic motion which is in line with the expectations.

5. Model correlation

The test case at 2000 RPM is considered. Post-processing of the HSC images of the top bearing (500 frames/sec) allows to evaluate several important parameters, e.g. $\alpha(t)$ (rotation angle of the cage), $\dot{\alpha}(t)$ (rotation speed of the cage), $x(t)$ and $y(t)$ (instantaneous coordinates of the cage centre). The following figures show a comparison of the MATLAB model with the measurements for the unlubricated case:

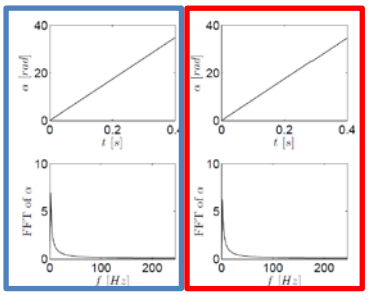

Model Test

Figure 17: α(t) from the model (left) and the test (right)

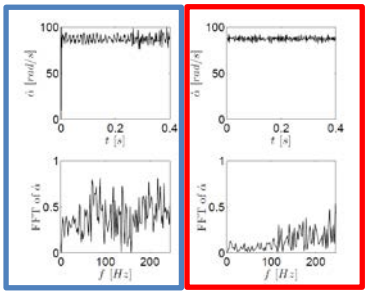

Model Test

Figure 18: $\dot{\alpha}$(t) from the model (left) and the test (right)

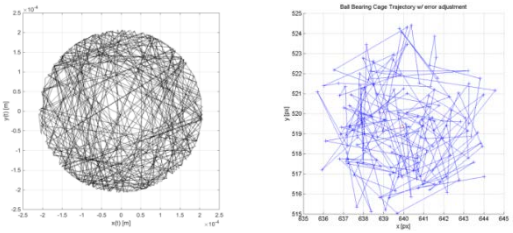

Model Test

Figure 19: Cage trajectory from the model (left) and the test (right)

Both in the test and in the model results, it is possible to observe the shaft's frequency (33 Hz) and the cage's frequency (13.5 Hz).

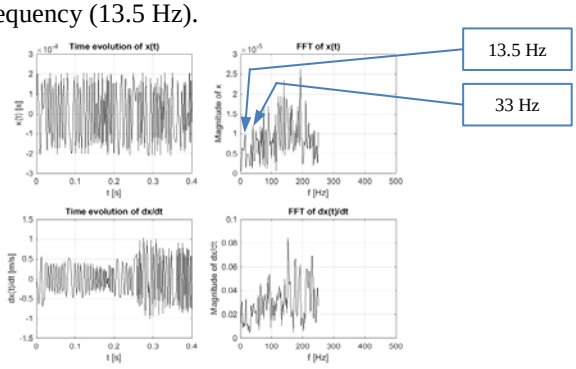

Figure 20: Main frequencies – shaft and cage (model)

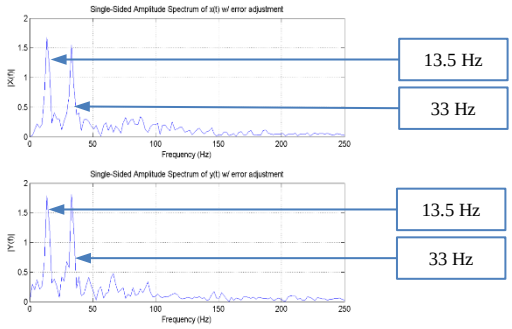

Figure 21: Main frequencies – shaft and cage (test)

The model appears to be more noisy with respect to the test results. It is believed that this could come from the damping coefficient (set arbitrarily to 50 N sec/m at both cage/races and cage/balls interfaces). Indeed, if the damping coefficient becomes 500 N·sec/m at the cage/ races (50 N sec/m are kept at the cage/ balls interface), the following improvement is obtained:

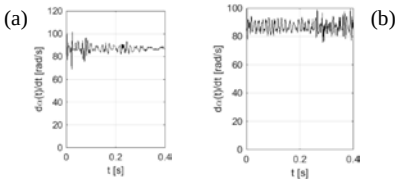

Figure 22: Numerical simulation results with 500N·sec/m damping at cage races (a) and 50 N·sec/m at cage races (b)

By comparing $\dot{\alpha}(t)$ with the previous simulation (with 50 N·sec/m damping coefficient at cage/races interface (Figure 22), it appears clear that more damping generates less noise in the model.

However, the impact on the centre of the cage trajectory is negligible.

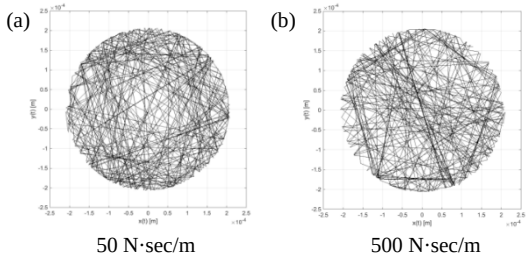

Figure 23: Trajectory for the increased damping coefficient (b)

6. Future perspectives

The relatively simple numerical model developed at ESA shows potential to predict the cage motion inside a ball bearing for space applications. The HSC appears to be a valuable tool to monitor the cage motion. It appears also that the model needs some upgrade, especially to:

- Improve the modelling of the contact (the model tends to be more noisy than the test).
- Have a more accurate check for the contact cage/balls (as explained in 2.3, when checking the described contact, the cage centre is considered to be located in the bearing's centre).

For that, a GSTP has been initiated with ULG to improve the MATLAB model and perform a more in-depth model correlation. In addition, there are the following relevant ongoing activities:

- ESA ARTES 5.1 activity initiated with AAC to develop a European material similar to well-known US materials (Duroid, PGM-HT).
- ESA TAP activity initiated with ESTL on the fundamentals of transfer film lubrication for cages made of self-lubricating materials. It is foreseen to evaluate, mainly by test, the typical wear of the European material developed under the ARTES 5.1 activity. This wear will depend on the number of contacts cage/ balls (which will be evaluated with the GSTP activity).

This will allow to set-up a life prediction model for a ball bearing's cage made with a self-lubricating European material. If this is achieved, it will be a breakthrough in mechanism and tribology science.

7. Conclusions

A preliminary model to predict the cage motion has been developed and correlated with the tests where ball bearing's cage was monitored with the High Speed Camera. Some improvements of the model are required. However, the following preliminary rules considering mainly the cage instability phenomena have been established (assuming speeds relevant for reaction wheels application – up to a few thousands RPM):

Parameter	Rule
Lubricant	Using a lubricant increases the stability
Preload	If the preload decreases, the stability increases
Number of balls	If the number of balls increases, the stability increases
Friction coefficient at cage/ races and cage/ balls	If the friction coefficient decreases, the stability increases
Speed	If the speed decreases, the stability increases
Ball diameter	If the ball diameter increases, the stability increases
$c = \frac{clearance(ball/pocket)}{clearance(cage/race)}$	When c < 1, in principle the cage is stable

Table 3: Influence of various parameters on cage's stability

8. REFERENCES

[1] A high precision instrument for analysing non-linear dynamic behaviour of bearing cage, Z.Yang, North West Polytechnic University, China

[2] Experimental study of a roller bearing kinematics through a high speed camera, S.Yunusov, Transport and Telecommunication Institute, Latvia

[3] M.Buttery, *Fundamentals of transfer film lubrication*, ESA Mechanisms Final Presentation Days (2017)